



**HAL**  
open science

# Influence of Water Addition on the Latent Heat Degradation of Sodium Acetate Trihydrate

Noé Beaupere, Ulrich Soupremanien, Laurent Zalewski

## ► To cite this version:

Noé Beaupere, Ulrich Soupremanien, Laurent Zalewski. Influence of Water Addition on the Latent Heat Degradation of Sodium Acetate Trihydrate. Applied Sciences, 2021, 11 (2), pp.484. 10.3390/app11020484. hal-03246444

**HAL Id: hal-03246444**

**<https://hal.science/hal-03246444v1>**

Submitted on 18 Jan 2023

**HAL** is a multi-disciplinary open access archive for the deposit and dissemination of scientific research documents, whether they are published or not. The documents may come from teaching and research institutions in France or abroad, or from public or private research centers.

L'archive ouverte pluridisciplinaire **HAL**, est destinée au dépôt et à la diffusion de documents scientifiques de niveau recherche, publiés ou non, émanant des établissements d'enseignement et de recherche français ou étrangers, des laboratoires publics ou privés.



Distributed under a Creative Commons Attribution 4.0 International License

1 Article

# 2 Influence of Water Addition on the Latent Heat 3 Degradation of Sodium Acetate Trihydrate

4 Noe Beaupere <sup>1,2,\*</sup>, Ulrich Soupremanien <sup>2</sup> and Laurent Zalewski <sup>2</sup>

5 <sup>1</sup> Université Grenoble Alpes, CEA Grenoble, CEA/LITEN/DTNM/SA3D/LMCM, 38000 Grenoble, France;  
6 ulrich.soupremanien@cea.fr (U.S.)

7 <sup>2</sup> Univ. Artois, Univ. Lille, Institut Mines-Télécom, Junia, ULR 4515 – LGCgE, Laboratoire de Génie Civil et  
8 géo-Environnement, F-62400 Béthune, France; laurent.zalewski@univ-artois.fr (L.Z.)

9 \* Correspondence: noe\_beaupere@ens.univ-artois.fr

10 Received: date; Accepted: date; Published: date

11 **Abstract:** To promote the development of thermal energy storage (TES), the sodium acetate  
12 trihydrate (SAT) presents interesting thermal properties. However, this material may suffer from  
13 aging throughout thermal cycles. Various solutions were explored in the literature to limit this  
14 aging, mainly based on the use of additives such as water. In this study, two samples were prepared.  
15 The first one consisted of raw SAT material whereas 3 wt.% of supplementary water has been added  
16 to the second one. They were then poured into 350 cm<sup>3</sup> bricks, which were placed in an experimental  
17 test bench. After 35 cycles between 20 and 70 °C, a drop of about 10 % of the latent heat was observed  
18 for the first sample. This behavior was similar to the literature data. For the second sample, the  
19 decrease of latent heat was more rapid (about 30%). Contrary to our expectations, the water addition  
20 seems not beneficial for the improvement of thermal stability. Interestingly, we noticed that the drop  
21 of the latent heat was fully reversible after sample stirring. This degradation might not be related to  
22 a thermal destructive mechanism but rather to a global segregation phenomenon. This segregation  
23 may be due to the breaking of hydrogen bonding between anhydrous sodium acetate and water,  
24 resulting in the separation of the two species.

25 **Keywords:** Thermal energy storage; Sodium acetate trihydrate; Aging study; Latent heat  
26 degradation and Water addition  
27

## 28 1. Abbreviations

Name	Symbol	Unit
Sodium Acetate Trihydrate	SAT	
Latent Heat	$L$	J.m <sup>-3</sup>
Mass	$m$	kg
Specific Heat Capacity	$C_p$	J.kg <sup>-1</sup> .K <sup>-1</sup>
Surface	$S$	m <sup>2</sup>
Temperature	$T$	K
Melting Temperature	$T_{melt}$	K
Mass Fraction of Sodium Acetate (CH <sub>3</sub> COONa)	$w_{SA}$	-
Heat Flux	$\phi$	W.m <sup>-2</sup>
Subscript		
Related to Solid	$x_S$	
Related to Liquid	$x_L$	

29

30

## 31 2. Introduction

32 Phase change materials (PCMs) appear as an attractive solution for thermal energy storage and  
33 for the development of renewable energies. Indeed, they can be used for both domestic hot water  
34 production [1] and passive heating/cooling of buildings [2]. For a better ratio of production vs.  
35 volume, daily melting and solidification are generally wished. Thus, many thermal cycles may be  
36 applied to the material that may suffer from aging, resulting in a decrease of the latent heat.

37 In particular, salt hydrates have an appropriate range of melting points (between -5 and +120 °C)  
38 for building applications and a range of interesting latent heat capacity (100-350 J.g<sup>-1</sup>) [3]. The solid  
39 phase of this class of PCMs presents a density of approximately 1700 kg.m<sup>-3</sup> and a specific heat  
40 capacity around 1650 J.kg<sup>-1</sup>.K<sup>-1</sup> [3], which may ensure relevant heat storage capabilities. One of the  
41 most interesting materials issued from this class of PCMs is sodium acetate trihydrate  
42 (SAT, CH<sub>3</sub>COONa·3H<sub>2</sub>O). However, the SAT may present a large supercooling degree up to 100 K [4].  
43 This high value of supercooling is generally perceived as a drawback but could be turned into a  
44 benefit if a reliable solidification triggering technique could be developed [3]. This would lead to the  
45 discharge of the stored heat on demand [5]. The heat release amplitude will depend on the triggering  
46 temperature (as losses may occur during the cooling of the supercooled SAT).

47 This quantity of stored heat in the supercooled SAT may be degraded by aging throughout  
48 successive thermal cycles, a process already explored for other PCMs [6,7]. As the SAT is heated until  
49 58 °C, an incongruent melting is observed according to the phase diagram [8] due to the break of  
50 hydrogen bonds. The SAT decomposes into two components: sodium acetate (CH<sub>3</sub>COONa) and water  
51 (H<sub>2</sub>O) that have different densities. If a temperature of 77 °C is reached, different behavior is observed  
52 upon cooling, with a solution (45.7wt% of water instead of 39.7wt%) and the segregation of sodium  
53 acetate. Kong *et al.* showed that the concentration of a non-stirred SAT mixture depends on the height  
54 in the container [9]. The separation of species will increase with cycles, as the mobility is limited both  
55 in liquid (no agitation) and in solid state as the remaining SAT in the middle-height will crystallize  
56 and hinder the contact between the two species. This would decrease the latent heat released by the  
57 material, leading to a reduction of its storage capacity. It was observed by Kong *et al.* [9] that a deeper  
58 container (more than 5 cm in height) would limit the gathering of the two components to again form  
59 a trihydrate material. The aging of the SAT was analyzed by several authors such as Pálffy *et al.* [10]  
60 who experienced that a raw sample of SAT had lost about a third of its initial value after 300 cycles.  
61 The evolution throughout more cycles (600 cycles) was also performed by Wada *et al.* [8], showing  
62 that aging could be reduced thanks to impurities.

63 Several solutions were investigated to limit this aging [8,11,12], and one of them (addition of  
64 water) was found interesting as it also decreases the solidification temperature and thus promotes  
65 the supercooling degree [4]. Indeed, aging would be limited by an excess of water from the extra  
66 water principle, a concept developed by Furbo *et al.* [13]. Then, this phenomenon was observed by  
67 Kong *et al.* [9,11] as they increased the quantity of water, moving its mass concentration in SAT from  
68 39.7 to 45.7wt% (0 to 6wt% extra water). A constant quantity of latent heat was released by the  
69 solidification of material even after 130 days of supercooling. Dannemand *et al.* [14,15] have shown  
70 that a sample of SAT with 48.7wt% of water (9wt% of extra water) can suffer from aging during  
71 thermal cycling. Indeed, it was observed a decrease of 8% of its latent heat, from 194 to 179 kJ.kg<sup>-1</sup>  
72 after 14 cycles. The same authors observed in [16] that a sample with 43.5wt% mass concentration of  
73 water (3.8wt% extra water) presented a decrease from 177 to 140 J.g<sup>-1</sup> (-21%) after 17 cycles, but no  
74 comparison was made with raw material.

75 Such a comparison was performed in this study. First, the properties of raw material, and their  
76 evolution throughout thermal cycles, were investigated. A sample containing an addition of water  
77 was then analyzed. In the one hand, because water addition can increase the supercooling degree,  
78 this would limit the appearance of a non-wished solidification and a subsequent heat release what  
79 is relevant for an application. The monitoring of aging was based on the measurement of latent heat  
80 accumulated and released throughout the successive phase change. In the other hand, as the  
81 supercooling was so stable in the sample having extra-water, a way of solidification triggering  
82 needed to be developed. Thus, a seeding method by contacting a welding rod to the supercooling

83 SAT was finally selected to induce solidification. As solidification could be triggered, it was possible  
84 to compare the degradation of the latent heat in both samples.

### 85 3. Materials and Methods

#### 86 3.1. Preparation of Macro-encapsulated Sodium Acetate Trihydrate Samples

87 The material characterized in this study was SAT (Sigma Aldrich, BioXtra, 99 % purity). Two  
88 different samples have been prepared:

- 89 • A reference sample (SAT60%) with a raw fraction of 60.3wt% of  $\text{CH}_3\text{COONa}$  for a  
90 comparison with the data from the literature.
- 91 • A second sample (SAT58%) where water was added. In addition to a limitation of  
92 aging, this concentration was expected to bring stability regarding the supercooling  
93 phenomenon [11].

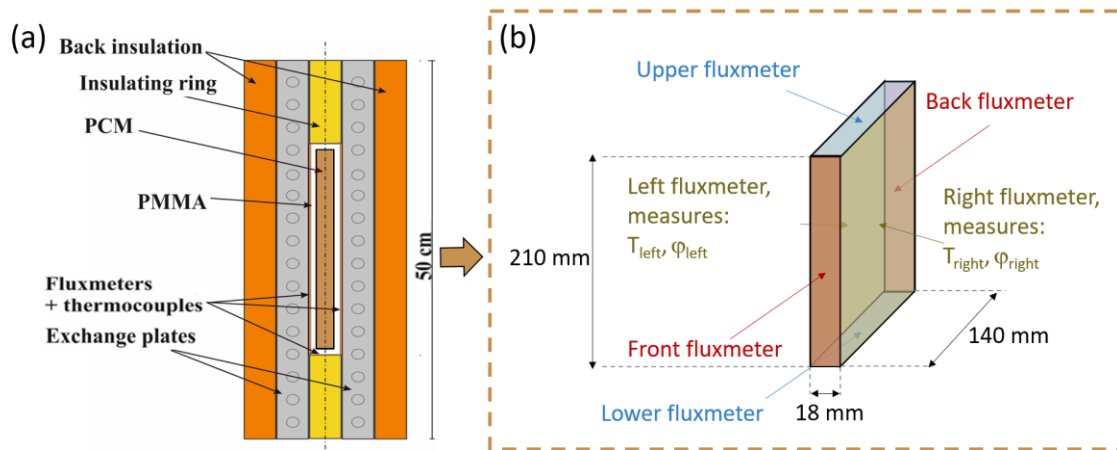
94 The samples were prepared from about 330 g of the raw material. For the second sample, the  
95 material was heated at a temperature of 70 °C for melting. This would allow for a better  
96 homogenization of the added deionized water (35 g). The sample was vigorously shaken to  
97 homogenize the repartition of water in the volume. The second sample was then solidified for  
98 transportation.

99 As they were solid, the real concentrations of both samples were measured. To do so, a  
100 ThermoGravimetric Analysis device (Netzsch, Pegasus 449 F1) was used. About 50 mg of material  
101 was taken from preparation and heated until 200 °C that was above the evaporation temperature of  
102 the water and allows for the analysis of a fully dry sample. For the SAT60% sample, the experiment  
103 was repeated 3 times for reliability, and the residual mass  $w_{SA}$  was included between 59.6wt% and  
104 61.5wt% (in comparison with a theoretical concentration of 60.3wt%). In the second sample, the  
105 experiments were repeated two times for reliability the residual mass of sodium acetate was found  
106 to be between 57.2 and 58.3wt%, for an average value of 57.7wt%. Such differences are assumed to  
107 be due to uncertainties.

108 After transportation, the samples were again melted for pouring by a syringe into 250 cm<sup>3</sup> bricks  
109 (210×140×18 mm<sup>3</sup>, 4 mm of thickness) that can contain 350 g of SAT. They were made of Polymethyl  
110 methacrylate (PMMA) that was found to have good chemical compatibility with SAT [17]. The bricks  
111 were sealed in order to limit the evaporation of water. The quantity of material was higher than the  
112 value used in the usual devices such as DSC (up to 40 μL) or calorimeter (about 10 mL). Its behavior  
113 is assumed to be more representative of that of a real system, having usually more than 1 L of PCM  
114 [18,19]. Once the material was solid, the brick was put into the experimental bench, and the analysis  
115 was launched.

#### 116 3.2. Experimental Set-up Description

117 The behavior of the material was studied by thermal cycling, which was considered to be  
118 representative of the behavior of a real application. This method is also the most currently used to  
119 study aging, according to Ferrer *et al.* [20]. However, these authors showed that mainly DSC devices  
120 or calorimeters were used. Therefore, a test ring that allows for better measurement of latent heat [17]  
121 was preferred in this work, (Figure 1 (a)). The sample was surrounded by fluxmeters where both heat  
122 flux and temperatures were measured (Figure 1 (b)). Therefore, the heat released by the sample was  
123 precisely recorded, which permits an adequate interpretation of the material behavior.



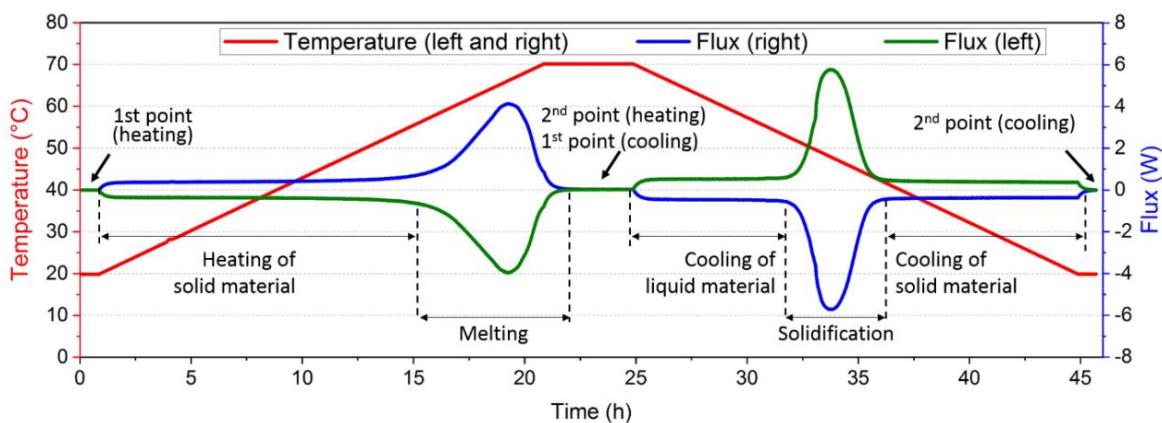
124  
125  
126

**Figure 1.** (a) Global description of the experimental bench and (b) focus on the sample, adapted from [21,22].

127 Two thermo-regulated water baths were used for temperature regulation of the exchange plates.  
 128 From preliminary experiments, it was observed that a heating and cooling rate of  $20\text{ }^{\circ}\text{C}\cdot\text{h}^{-1}$  gives  
 129 repeatable conditions between left and right plates ( $\pm 0.1\text{ }^{\circ}\text{C}\cdot\text{h}^{-1}$ ) and throughout cycles. This cooling  
 130 rate was chosen and thermal cycles of 8 hours were applied from  $20$  to  $70\text{ }^{\circ}\text{C}$ . The maximal  
 131 temperature was chosen to be above the melting temperature, approximately  $58\text{ }^{\circ}\text{C}$  for the SAT  
 132 compositions considered here according to Green [23]. This temperature was also chosen below  $77\text{ }^{\circ}\text{C}$   
 133 [24] to ensure the occurrence of solidification on the next cooling, which allows for the experimental  
 134 determination of the latent heat. In parallel, it was observed that the SAT generally solidifies around  
 135  $50\text{ }^{\circ}\text{C}$  in the prior experiments, therefore a minimal temperature close to the ambient conditions  
 136 ( $20\text{ }^{\circ}\text{C}$ ) was arbitrarily chosen.

137 **3.3. Data Analysis**

138 The thermal behavior of the material during a full cycle (heating, cooling, and constant  
 139 temperature steps), using the previously presented experimental bench, is described in Figure 2.  
 140 Whereas all the surfaces are covered by sensors, only the record of the left and right fluxmeters ( $140 \times$   
 141  $210\text{ mm}^2$ ) is given. Indeed, the measurements of the four other surfaces are not considered significant  
 142 as they represent about 4% of the total heat flux recorded.



143  
144

**Figure 2.** Description of a full thermal cycle.

145 Here, the analysis was performed between two points (1<sup>st</sup> and 2<sup>nd</sup> point) on both sides of a  
 146 temperature variation (heating or cooling). These two points were chosen at the end of the thermal  
 147 plateau in order to have a stabilized heat flux. Hence, a baseline below  $0.01\text{ W}$  could be obtained. The  
 148 value of latent heat could then be obtained from an integration of the heat flux between these two  
 149 points, after subtracting the sensible heat.

150 This sensible heat was stored in the container, made of PMMA, whose specific heat capacity  
 151  $C_{p,brick}$  has been determined by blank tests to be approximately  $1.45 \text{ kJ.kg}^{-1}.\text{°C}^{-1}$ . The sensible heat  
 152 was also stored in the solid  $C_{p,S}$  and liquid  $C_{p,L}$  SAT's specific heats. They can be calculated using  
 153 linear approximations, given in Eq. 1, based on the data from Araki *et al.* [25]. These equations were  
 154 considered valid for a mass fraction  $w_{SA}$  from 54.3 to 60.3wt% and a temperature between 27 and  
 155  $58 \text{ °C}$  for solid and between 27 and  $77 \text{ °C}$  for liquid (valid also in supercooled state), with an error of  
 156 5% maximum.

$$C_p = A + B T + (C + D T) w_{SA} \quad (1)$$

157 Where  $T$  is the temperature ( $\text{°C}$ ). The empirical parameters A, B, C, and D are given in Table 1 for  
 158 both solid and liquid specific heats.

159 **Table 1.** Empiric parameters for solid and liquid specific heat determination.

	A ( $\text{J.kg}^{-1}.\text{°C}^{-1}$ )	B ( $\text{J.kg}^{-1}.\text{°C}^{-2}$ )	C ( $\text{J.kg}^{-1}.\text{°C}^{-1}$ )	D ( $\text{J.kg}^{-1}.\text{°C}^{-2}$ )
$C_{p,S}$	3367	-10.74	-2412	24.67
$C_{p,L}$	4091	5.8	-2274	-2.52

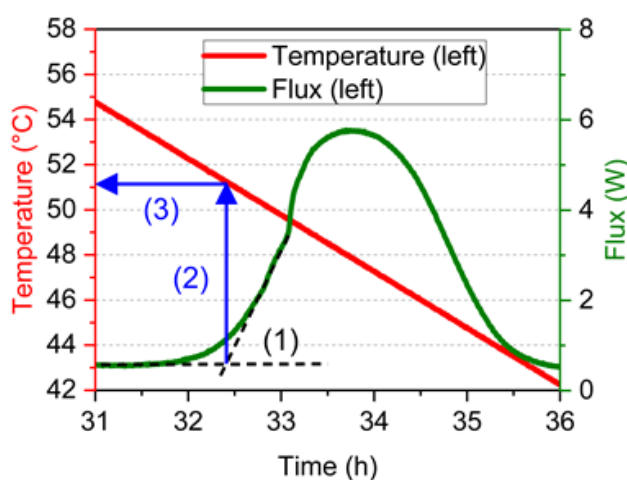
160 These two specific heats allow for the calculation of the latent heat. This evaluation is based on  
 161 the subtraction of the sensible energies to the global heat flux measured on the different surfaces, as  
 162 shown in Eq. 2.

$$L = \int_S \int_{t_1}^{t_2} \phi \, dt \, dS - \int_{20}^{70} m C_{p,brick} dT - \int_{20}^{T_{melt}} m C_{p,sol} dT - \int_{T_{melt}}^{70} m C_{p,liq} dT \quad (2)$$

163 Where  $t_1$  and  $t_2$  are the time for the 1<sup>st</sup> and 2<sup>nd</sup> point (Figure 2), and  $T_{melt}$  is the melting  
 164 temperature ( $58 \text{ °C}$ ). Eq. 2 is focused on the melting of the material because it was assumed that the  
 165 energy released during solidification was influenced by the possible presence of a non-repeatable  
 166 supercooling degree. This equation could be compared with an empirical relation from Araki *et al.*  
 167 [25], given in Eq. 3 that is valid for a mass fraction of sodium acetate  $w_{SA}$  from 47.5 to 60.3wt% with  
 168 an error of 5% maximum.

$$L = -462 + 11.8 w_{SA} \quad (3)$$

169 Moreover, the determination of the crystallization temperatures was necessary for a correct  
 170 analysis of the material's solidification and its impact on the next melting. For each cycle (as presented  
 171 in Figure 2), the onset temperature was determined in three steps. (1) The onset time was determined  
 172 by the intersection of 2 tangents represented by black dash lines in Figure 3. (2) The crystallization  
 173 temperature was then identified by a blue arrow and (3) its value was read on the left axis.



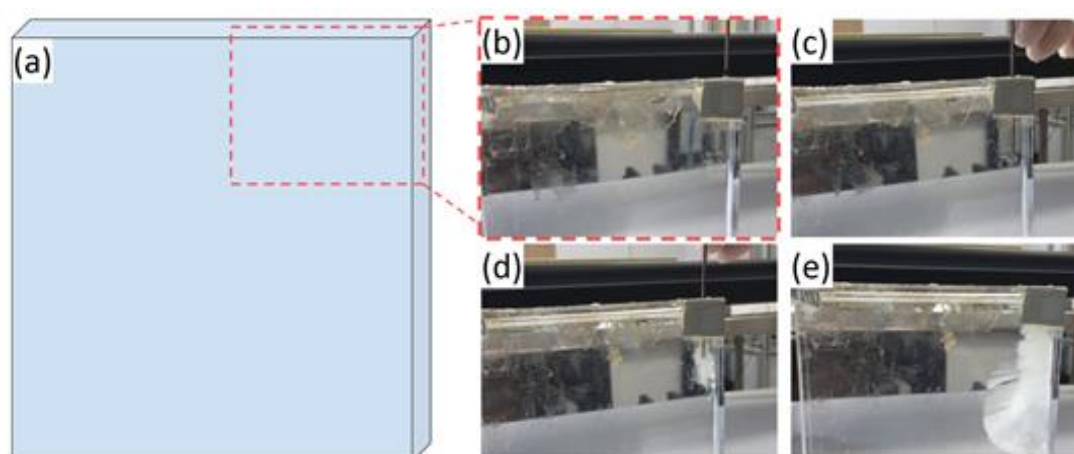
174 **Figure 3.** Method for crystallization onset temperature determination.

175  
 176 This procedure was then applied to the study of the two samples (SAT60% and SAT58%).

177 **4. Aging Study of Sodium Acetate Trihydrate**

178 *4.1. Experimental Validation of the Empirical Equations*

179 The validity of the previous equations was verified by the application of heating and cooling  
 180 cycles on a fully solid (between 20 and 28 °C) and fully liquid (between 63 and 70 °C) SAT60% sample.  
 181 During these tests, the supercooling state was not observed in this sample as the necessary conditions  
 182 were not reached. However, the supercooling degree in the SAT58% was increased by the addition  
 183 of water (reduction of the temperature of solidification) as noted by Wada *et al.* [4]. Experimentally,  
 184 the SAT58% sample did not crystallize even at a temperature as low as 5 °C. As the solidification was  
 185 not obtained by a temperature reduction, it was decided to trigger it by an external mean (insertion  
 186 of a copper welding rod), as presented in Figure 4.



187  
 188 **Figure 4.** Seeding of SAT with a welding rod (a) Schematic draw of the brick and detailed pictures  
 189 (after the brick was taken out of the experimental bench) (b) initial state; (c) insertion throughout the  
 190 grey tape; (d) beginning of crystallization and (e) growth of the crystal.

191 The crystallization of the supercooled SAT was observed after the introduction of this additional  
 192 metal rod. In addition, it continues appearing in the following cycles even after the rod had been  
 193 removed. As SAT may corrode copper [26], some particles were assumed to be spread in the liquid  
 194 PCM. These particles may act as nucleating agents as a new surface was provided from where the  
 195 nuclei would grow as lower energy is required [3]. Therefore, the addition of a small number of  
 196 particles can strongly promote the solidification of the SAT. This repeatable crystallization allows  
 197 performing preliminary thermal cycles with a phase change. The values of the latent heat, completed  
 198 by the specific heats measured for the SAT60% (solid and liquid) and the SAT58% (supercooled), are  
 199 given in Table 2. Indeed, the characterization of SAT58%, which was performed before the triggering  
 200 of the solidification by a metal rod, only gave properties for the supercooled state. The uncertainties  
 201 were calculated to include 99.7% of the values ( $\pm 3\sigma$ ). The number of experiments for each  
 202 measurement was also added.

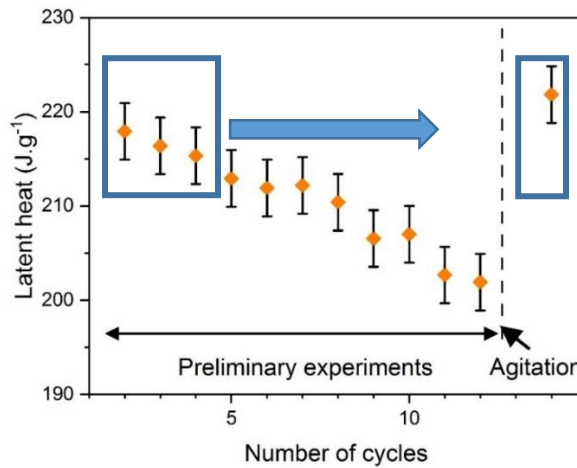
203 **Table 2.** Initial properties of the sample before aging.

	SAT58%	Number of experiments	SAT60%	Number of experiments
Mean $L$ value ( $J \cdot g^{-1}$ )	$214 \pm 3$	5	$253 \pm 2$	3
Difference with Eq. 3 (%)	2		1	
Mean $C_{P,S}$ value (20; 28 °C, $J \cdot kg^{-1} \cdot ^\circ C^{-1}$ )			$2021 \pm 19$	4
Difference with Eq. 1 (%)			0.2	
Mean $C_{P,L}$ value (63; 70 °C, $J \cdot kg^{-1} \cdot ^\circ C^{-1}$ )			$3260 \pm 35$	4
Difference with Eq. 1 (%)			9.3	
Mean $C_{P,supercooled}$ value (5; 70 °C, $J \cdot kg^{-1} \cdot ^\circ C^{-1}$ )	$3199 \pm 15$	10		
Difference with Eq. 1 (%)	8			

204 The measured specific heat was found consistent with the literature data [25] as a difference of  
 205 less than 10% was found regarding Eq. 1. The same observation was done for the latent heat  
 206 determined from Eq. 2 (maximal difference 2% regarding Eq. 3 from the literature). Nevertheless,  
 207 only a few experiments could be performed, as they may induce the aging of the sample.

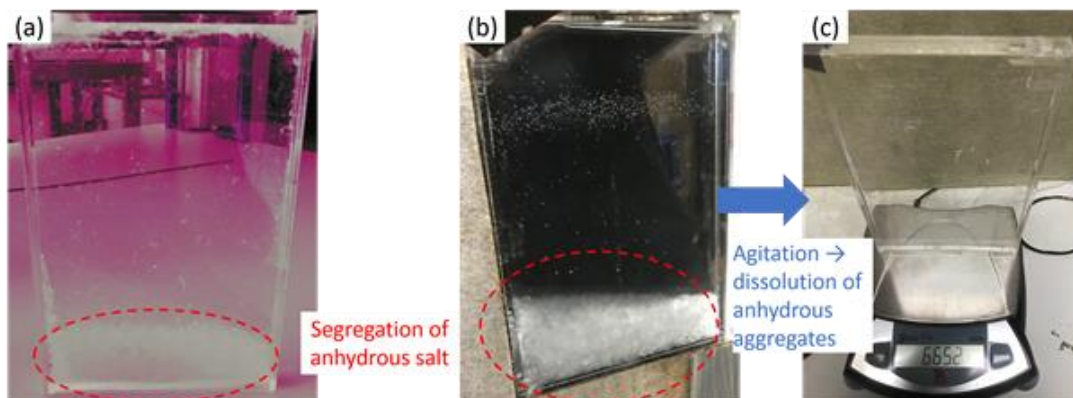
208 **4.2. The Initial Drop of Latent Heat During Preliminary Cycles**

209 In order to verify the repeatable apparition of solidification and melting before the aging  
 210 analyses and compare the measured latent heat with Eq. 3, preliminary cycles were performed on  
 211 SAT58%. From Eq. 2, the latent heat of melting could be determined and its evolution is given in  
 212 Figure 5. The uncertainties are given in Table 2.



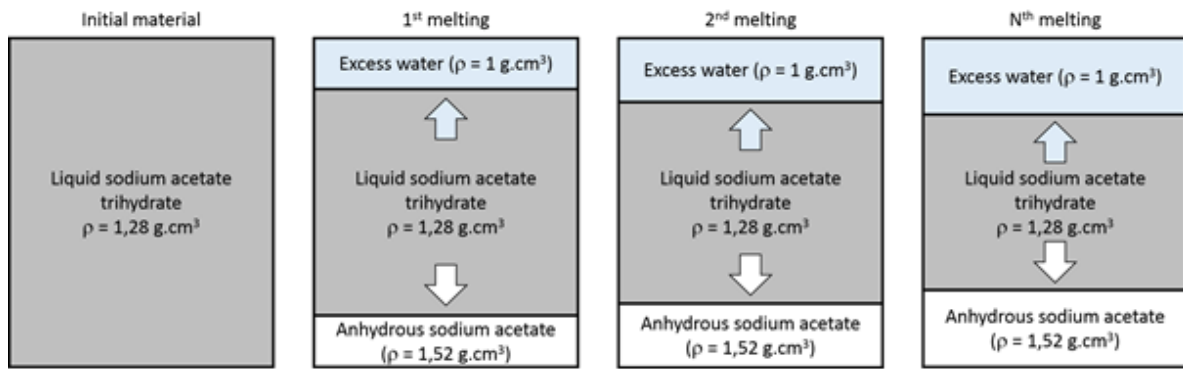
213  
 214 **Figure 5.** Preliminary evaluation of latent heat of SAT58%. The arrow symbolizes a reset of the  
 215 properties by agitation (the two rectangles allow for comparison of the latent heat at the beginning of  
 216 the experiment and after agitation).

217 It was observed that a phase change (melting and solidification) occurred at every preliminary  
 218 cycle. In the 3 first cycles (left blue rectangle), the latent heat determined by Eq. 2 differed by a  
 219 maximum of 2% from Eq. 3 from Araki *et al.* [25]. However, it was suspected that these preliminary  
 220 thermal cycles had induced the aging of the material. Indeed, a decrease of the latent heat from 220  
 221 to 200 J.g<sup>-1</sup> was observed after 12 thermal cycles. In parallel, the bricks containing the different  
 222 samples were taken out of the experimental bench at the end of the preliminary stage. The segregation  
 223 of anhydrous salt could be observed at the bottom of the brick. This segregation can either be due to  
 224 the melting before the filling of the brick (SAT60%, Figure 6 (a)) or the preliminary aging cycles  
 225 (SAT58%, Figure 6 (b)).



226  
 227 **Figure 6.** Formation of anhydrous salt segregation in (a) SAT60% (the colors were modified for  
 228 contrast accentuation), (b) SAT58%, and (c) SAT58% after agitation, before insertion in the  
 229 experimental bench.

230 According to the phase diagram of Sodium Acetate - Water [23], a peritectic transformation exist  
 231 during melting of the material for a concentration above  $w_{SA} = 0.57$ . This transformation is  
 232 associated with the formation of anhydrous salt and water. Indeed, these two molecules are linked  
 233 in SAT by a hydrogen bond [27] that can easily be broken. The anhydrous sodium acetate, denser,  
 234 may fall at the bottom of the brick, whereas water is generally found in the upper part [9]. Thus, the  
 235 quantities of water and anhydrous salt are increased in the global volume, as presented in Figure 7.  
 236 This phenomenon of aging continues with cycles and reduces the capacity of the global volume to  
 237 release the latent heat.



238  
239

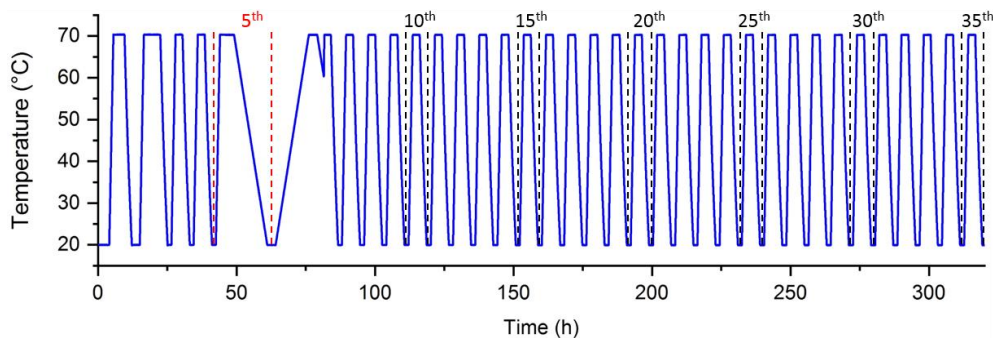
**Figure 7.** Schematic diagram of SAT aging throughout melting cycles.

240 Thus, it can be considered that the height of the sample also influences aging. As experimented  
 241 by Kong *et al.* [9], a sample with a height of 8 cm was more subjected to aging than other samples of  
 242 4 or 5 cm. Indeed, the gravity phenomenon and the separation of species would be accentuated for  
 243 samples of important heights. In existing application prototypes (250 L) the heights of the cells were  
 244 limited to 5 cm height to reduce the separation phenomenon [19].

245 As it was observed that the latent heat could be regenerated by agitation, the bricks were then  
 246 vigorously shaken by hands. This results in a visual elimination of segregation as presented in Figure  
 247 6 (c). This can be correlated to the fact that the latent heat measured on the following thermal cycle  
 248 (after agitation) was similar to the initial value of the sample. The agitation, that was here manual,  
 249 could be done by mechanical means such as nucleation triggering technique like ultrasounds [3] or  
 250 bubbling [28]. This solution may also allow the release of heat on demand by inducing the  
 251 solidification of a supercooled SAT. After the segregated salt had been dissolved by shaking, the  
 252 bricks containing the different SAT samples were then ready for aging analysis.

253 **4.3. Study of the Raw Material (SAT60%)**

254 To evaluate the potential of the use of water in order to attenuate the aging of the SAT, the  
 255 behavior of raw material was first evaluated. Therefore, 35 cycles between 20 and 70 °C were applied  
 256 to the sample. These cycles may be summarized in Figure 8. It may be noted that a discontinuity  
 257 appears between the 5<sup>th</sup> and 6<sup>th</sup> cycle that corresponds to the change of heating and cooling rate.

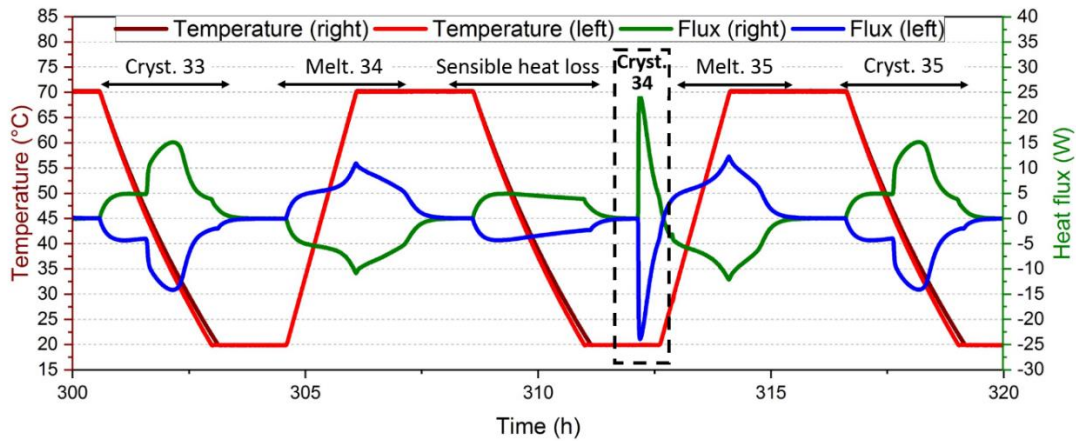


258  
259

**Figure 8.** Temperature evolution along the experiment performed on SAT60%.

260 The 1<sup>st</sup> cycle of the series was not considered here because of a different thermal history. Besides,  
 261 some cycles were applied with a different heating and cooling rate (5<sup>th</sup> cycle) whose results were used  
 262 in another study [19]. This lead to a different thermal history for the 6<sup>th</sup> cycle. Therefore, 1<sup>st</sup>, 5<sup>th</sup>, and  
 263 6<sup>th</sup> were not considered in the analysis and plotted as stars in the following graphs to perceive the  
 264 influence of different experimental parameters.

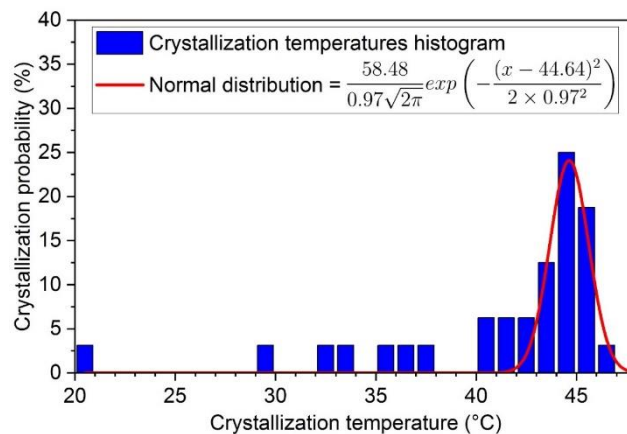
265 The latent heat of the remaining cycles could be determined from Eq. 2, leading to the monitoring  
 266 of aging. However, some crystallizations that occurred at a lower temperature would influence the  
 267 latent heat measurement, such as the 34<sup>th</sup> cycle of this experiment, which is plotted in Figure 9.



268  
 269 **Figure 9.** Singular crystallization at 20 °C for the 34th cycle of the experiment. Cryst.: Crystallization.  
 270 Melt.: Melting.

271 During this 34<sup>th</sup> crystallization, the heat flux was not stabilized and the core of the material may  
 272 still be cooling as the temperature started to re-increase. As the material remained hot, the energy  
 273 needed to bring the material back to 70 °C for the 35<sup>th</sup> melting may be lowered. In parallel, it was  
 274 assumed in the calculation of the sensible heat subtracted (Eq. 2) that the whole material was heated  
 275 from 20 to 70 °C. Therefore, the latent heat, determined from Eq. 2 during the 35<sup>th</sup> melting, may be  
 276 underestimated. Even if this is an extreme case, the next melting may be impacted by a delay in the  
 277 solidification of singular points. Besides, a faster solidification was observed when the supercooling  
 278 degree was larger [29]. This may induce a larger number of porosities [30] and influence its properties  
 279 and the progression of the melting front on the next heating step. For these reasons, the melting that  
 280 follows a low-temperature crystallization has been considered as singular data.

281 Before the determination of latent heat, the first step was to measure the crystallization  
 282 temperatures, based on the procedure given in Figure 3. The histogram of crystallization  
 283 temperatures is given in Figure 10 with a step of 1 °C, where the values for the 1<sup>st</sup>, 5<sup>th</sup>, and 6<sup>th</sup> cycles  
 284 are excluded.



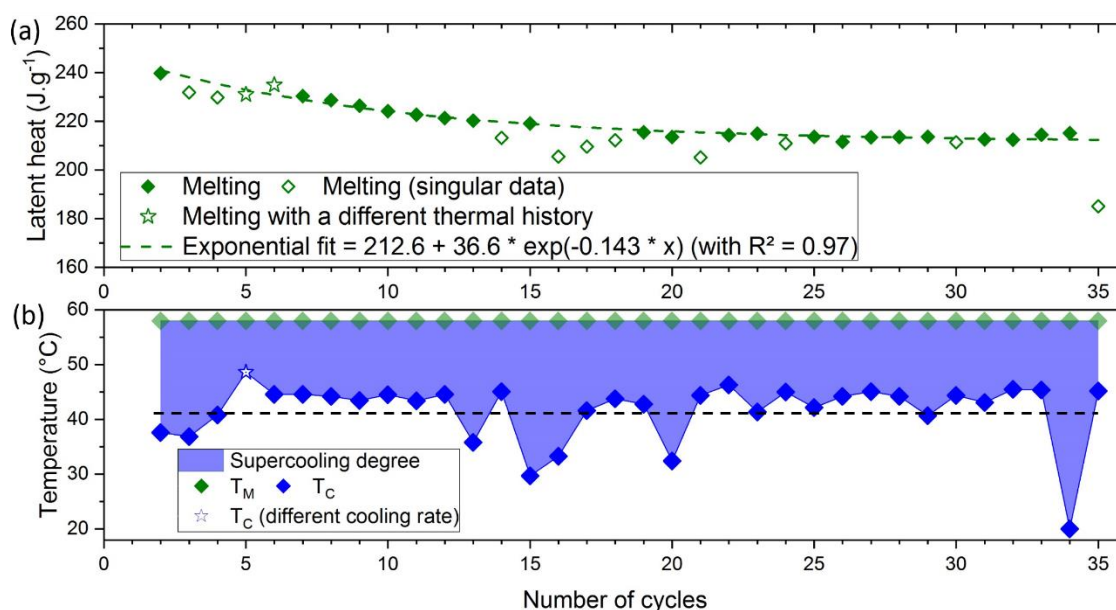
285  
 286 **Figure 10.** Probability distribution of crystallization temperatures for SAT60%.

287 It can be seen that the crystallization temperatures are not homogeneous, but they can be  
 288 approximated by a normal distribution (in red). The mean value  $T_{C,mean}$  is here equal to 44.64 °C and  
 289 the standard deviation  $\sigma$  is about 0.97 °C. The crystallization temperatures out of a range of  
 290  $T_{C,mean} \pm 3\sigma$  ( $T_C < 41.7$  °C) were considered as singular data. In the present case, about 11 over a  
 291 total number of 32 solidifications (34%) were concerned, after the exclusion of 1<sup>st</sup>, 5<sup>th</sup>, and 6<sup>th</sup> cycles.

292 The second step consisted of the latent heat monitoring for these non-singular points. Its  
 293 evolution throughout cycles is given in Figure 11 (a). The singular data (open symbols) were  
 294 separated from other values of latent heat, whose decrease should only be related to aging. However,  
 295 a fluctuation in the remaining crystallization temperatures (between 41 and 47 °C) was still noticed,  
 296 and the latent heat of the next melting may still be influenced. It was assumed from Figure 7 that the  
 297 quantity of SAT was decreasing throughout cycles. This led to the assumption that the probability of  
 298 a SAT's molecule to be separated (into water and anhydrous sodium acetate) was constant. This is  
 299 characteristic of an exponential decrease fit. To find a trend of aging, the latent heat for non-singular  
 300 data were fitted by an exponential decrease law (dashed curve), given in Eq. 4.

$$\frac{dL(x)}{dt} = -b L(x) \quad (4)$$

301 where  $L(x)$  is the latent heat for any cycle  $x$ . The crystallization temperatures are also plotted at the  
 302 bottom (Figure 11 (b)). Thus, the relation between singular crystallization temperatures (below the  
 303 black dashed curve) and lower latent heat values on the next cycle (open symbol) would be  
 304 highlighted.



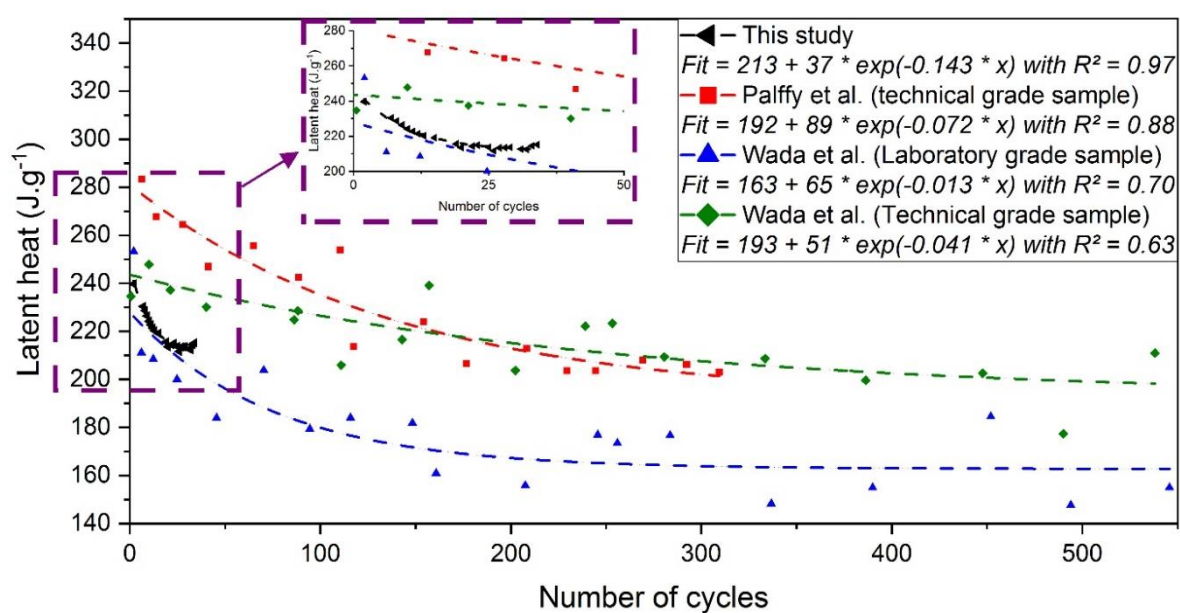
305

306 **Figure 11.** Evolution of (a) the latent heat and (b) the supercooling degree over 35 cycles of a raw SAT  
 307 sample ( $w_{AS} = 0.603$ ). Values for the 5<sup>th</sup> and 6<sup>th</sup> symbol (from different thermal history) are plotted as  
 308 stars. The open symbols (following a low-temperature crystallization) will not be considered for  
 309 exponential fit and aging analysis.  $T_M$  and  $T_C$  respectively represent melting and crystallization  
 310 temperatures.

311 In addition to the 5<sup>th</sup> cycle that was cooled more slowly (2.5 °C.h<sup>-1</sup> instead of 20 °C.h<sup>-1</sup>) and  
 312 crystallized at a higher temperature (50 °C), several singular points ( $T_C < 41.7$  °C) were observed.  
 313 The gap between those temperatures and the mean one seems to increase throughout cycles. Indeed,  
 314 it was low at the beginning, with a crystallization temperature of 38 °C (a supercooling degree  
 315  $\Delta T \approx 28$  °C) different from the mean value of 45 °C ( $\Delta T \approx 13$  °C). Then, an increase in the gap was  
 316 found over the number of cycles as a crystallization temperature of 30 °C ( $\Delta T = 28$  °C) is reached  
 317 after the 15<sup>th</sup> cycle and is minimal after the 34<sup>th</sup> cycle (crystallization temperature of 20 °C ( $\Delta T \approx$   
 318 38 °C)). This increase of the gap directly impacts the latent heat and may be related to aging as the

319 quantity of material presenting a stoichiometric concentration ( $w_{AS} = 0.603$ ) decreases over cycles. It  
 320 is assumed that this reduction of volume would lead to the reduction of the number of potential sites  
 321 for nucleation of the SAT and the rise of the supercooling degree. This was supported by the work of  
 322 Guion *et al.* [31], who noticed an increase of this supercooling degree throughout the aging cycle of  
 323 the SAT.

324 Without considering these singular crystallizations, the latent heat on the second cycle was about  
 325  $240 \text{ J.g}^{-1}$ , close to literature data [25,32]. Then, the latent heat decreases and stabilizes around  $213 \text{ J.g}^{-1}$   
 326 after 35 cycles, which represents a drop of about 10%. A comparison was done with the results from  
 327 other studies, performed over more cycles. Figure 12 presents the evolution of latent heat throughout  
 328 aging from Pálffy *et al.* [10] and Wada *et al.* [33], combined with the results obtained from SAT60%.  
 329 The exponential decrease fits from the data of the different authors are represented by dashed curves.



330

331 **Figure 12.** Evolution of latent heat adapted from Pálffy *et al.* [10] (in red), Wada *et al.* [8] for a technical  
 332 grade (in green), and laboratory-grade (in blue) combined with the results obtained here (in black).  
 333 The symbols represent the value obtained by authors. The dashed line corresponds to the exponential  
 334 fit that was performed in this study. An inset is given from 0 to 50 cycles.

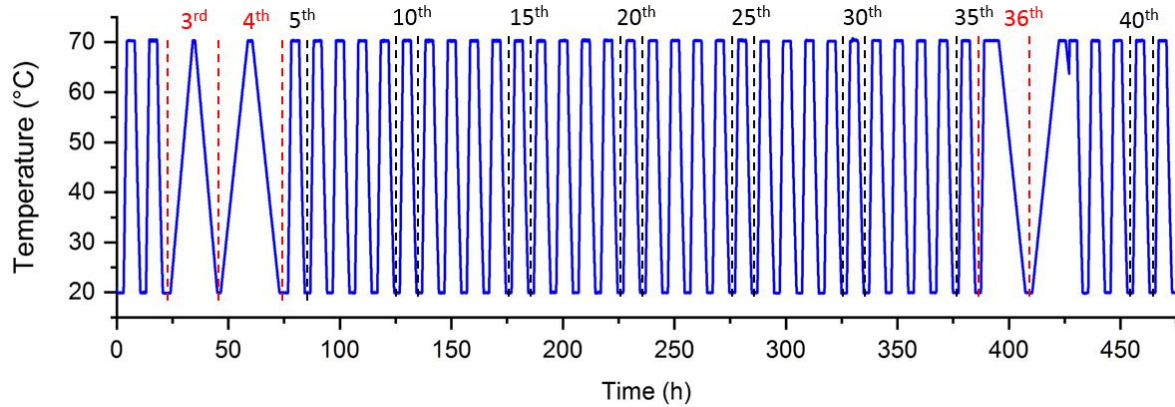
335 The sample tested here presents an initial latent heat around  $240 \text{ J.g}^{-1}$  that reaches approximately  
 336  $213 \text{ J.g}^{-1}$  (-11%) after 35 cycles applied between 20 and  $70 \text{ }^\circ\text{C}$ . In comparison, an analysis performed  
 337 by Wada *et al.* [8] (green curve) showed that the latent heat of the SAT technical-grade sample seemed  
 338 to stabilize around  $200 \text{ J.g}^{-1}$  (-17.4%) after 300 cycles applied between 40 and  $70 \text{ }^\circ\text{C}$ . The results were  
 339 comparable for Pálffy *et al.* [10] (red curve) where a drop of the latent heat from 280 to  $200 \text{ J.g}^{-1}$   
 340 (-28.5%) of a SAT technical grade sample was found after 300 cycles applied between 23 and  $65 \text{ }^\circ\text{C}$ .  
 341 Besides, Wada *et al.* have tested a laboratory-grade sample (blue curve) where aging was stronger, as  
 342 latent heat in the range from 150 to  $170 \text{ J.g}^{-1}$  was reached after 300 cycles. It was assumed by [8] that  
 343 the impurities, which are more present in the technical-grade sample, may be absorbed onto the  
 344 surface of anhydrous salt particles and limit their aggregation.

345 A high drop of latent heat was obtained in the first cycles for the sample tested (99% purity),  
 346 similar to the laboratory-grade sample (blue curve) of Wada *et al.* Then, it differs from the blue curve  
 347 after about 20 cycles, as the exponential fit stabilized around  $213 \text{ J.g}^{-1}$ . Moreover, it can be observed  
 348 that the  $R^2$  values are higher in this study. This shows the efficiency of the particular experimental  
 349 bench in the determination of a consistent value of the latent heat stored.

350 As a conclusion, the aging behavior of SAT60% is roughly similar to the literature data. It  
 351 appeared that this decrease of the latent heat is important and cannot be neglected in the development  
 352 of applications. The addition of water as a solution to aging would then be studied.

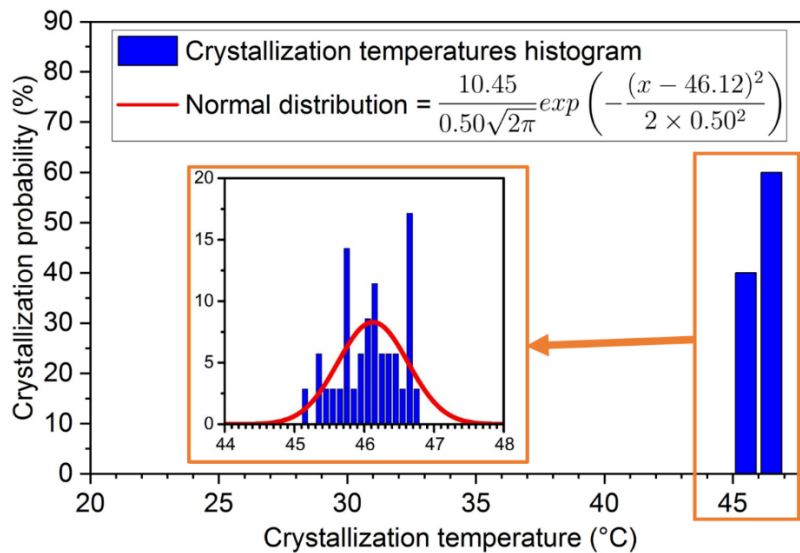
353 4.4. Resistance to the Aging of a Sample Having Additional Water

354 To evaluate the influence of water on the aging of SAT, similar cycles were applied to the  
 355 SAT58% sample. For better clarity, the temperature evolution of this experiment is given in Figure  
 356 13.



357  
 358 **Figure 13.** Evolution of temperature throughout aging cycles.

359 As before, the 3<sup>rd</sup>, 4<sup>th</sup> and 36<sup>th</sup> cycles, whose heating and cooling rate were about 2.5 °C.h<sup>-1</sup>, were  
 360 dedicated to the study of latent heat evolution under different conditions [19]. Due to their different  
 361 thermal history, the data could not be included in the global analysis and will be later plotted as stars.  
 362 This also concerns the 5<sup>th</sup> and 37<sup>th</sup> cycles, whose thermal history was impacted by the previous heating  
 363 and cooling steps. These five cycles were not considered for the probability distribution of the  
 364 crystallization temperatures that are presented in Figure 14 with a 1 °C step.

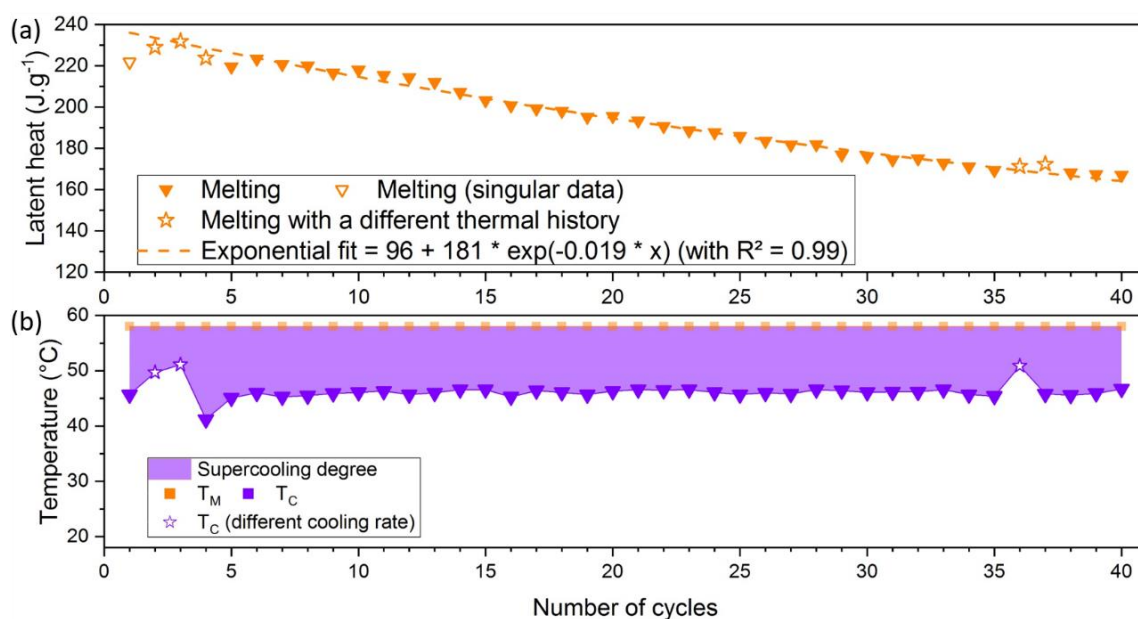


365  
 366 **Figure 14.** Probability distribution of crystallization temperatures for SAT58%. In the inset, the  
 367 crystallization temperature has a 0.1 °C temperature step.

368 Better repeatability of the crystallization temperature was found in these 35 cycles (after  
 369 exclusion of the 1<sup>st</sup>, 3<sup>rd</sup>, 4<sup>th</sup>, 5<sup>th</sup>, 36<sup>th</sup>, and 37<sup>th</sup>) with values between 45 and 47 °C. It can be noted that  
 370 the temperature distribution is more homogeneous. As shown in Figure 4, a copper welding rod was  
 371 previously inserted in the liquid SAT58%. Copper may have been corroded by SAT and particles may  
 372 be present in the SAT's solution, promoting the solidification of the material.

373 The mean temperature obtained was  $T_C = 46.1$  °C, with a standard deviation  $\sigma = 0.5$  °C. The  
 374 whole crystallization temperatures are included in the distribution range and the consideration of

375 singular points would not be needed for this SAT58% sample. The evolution of the latent heat  
 376 throughout cycles was then determined, and the results are shown in Figure 15.



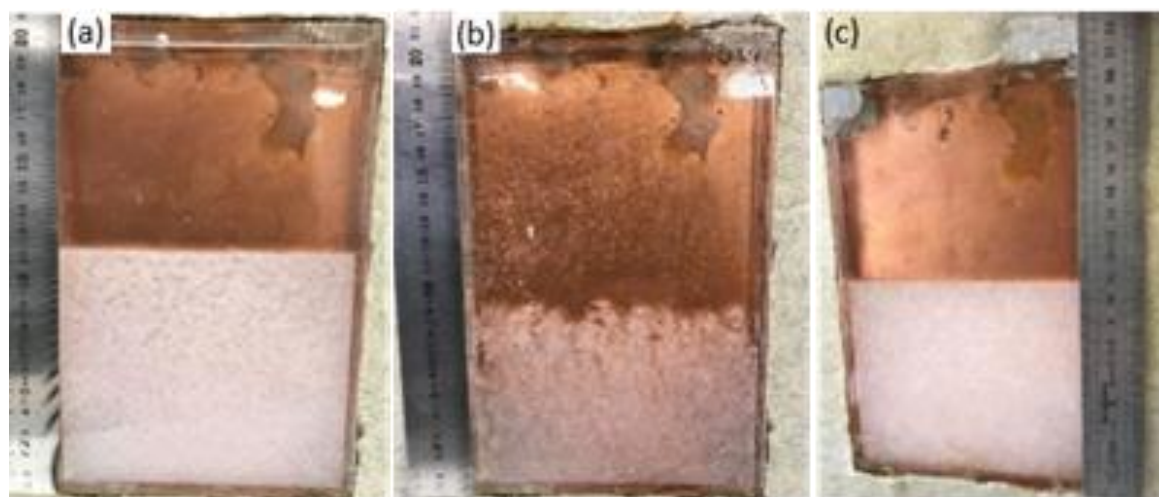
377  
 378 **Figure 15.** Evolution of (a) the latent heat and (b) the supercooling degree over 40 cycles of a SAT58%  
 379 sample ( $w_{SA} = 0.577$ ). Values for 3<sup>rd</sup>, 4<sup>th</sup>, 5<sup>th</sup>, 36<sup>th</sup>, and 37<sup>th</sup> are plotted as stars. As the open symbols  
 380 (following a low-temperature crystallization), they will not be considered for exponential fit and  
 381 aging analysis.  $T_M$  and  $T_C$  respectively represent melting and crystallization temperatures.

382 This sample presents an initial latent heat between 220 and 230 J.g<sup>-1</sup> while the first cycles are  
 383 difficult to consider due to a different thermal history. The trend is more obvious for this sample  
 384 containing an addition of water, with a coefficient of determination  $R^2 = 0.99$ . The decrease of latent  
 385 heat is also more important, up to 25% of its initial value throughout 35 cycles, and continues for the  
 386 5 remaining cycles. Besides, this trend was verified for a slower cooling rate (2.5 °C.h<sup>-1</sup>) for the 3<sup>rd</sup>, 4<sup>th</sup>  
 387 and 36<sup>th</sup> cycles, plotted as stars. Their crystallization temperatures were closed to each other  
 388 (respectively 49.7 °C, 51.1 °C and 50.9 °C). This behavior was similar to the observations of  
 389 Dannemand *et al.* [14] where a decrease of 8% (from 194 to 179 J.g<sup>-1</sup>) was found after 20 cycles for a  
 390 concentration  $w_{SA}=56.5\text{wt}\%$ .

391 The water addition, rather than increasing the aging stability of the SAT as proposed by Kong *et*  
 392 *al.* [9], tends to diminish it. Then, to explain the behavior of the different samples, visual observations  
 393 of the aged samples were performed.

## 394 5. Discussion on the Visual Aspect of the Samples

395 After the thermal cycles were applied to the different samples, they were taken out of the  
 396 experimental bench, without shaking to avoid the contact between anhydrous salt and water. It was  
 397 first noted that a large quantity of anhydrous salt had segregated at the bottom of the box, as  
 398 presented in Figure 16. For SAT58%, some cycles were done at a higher temperature (80 °C). To take  
 399 this into account, a picture of SAT60% that has undergone similar temperature cycles (up to 80 °C)  
 400 was also added for better comparison.



401  
 402 **Figure 16.** Visual appearance of (a) SAT60% after 35 cycles at 70 °C, (b) the same sample after 46 more  
 403 cycles until 80 °C and (c) SAT58% after 41 cycles until 70 °C and 10 cycles until 80 °C.

404 The height of the anhydrous sodium acetate aggregate, considered as an indicator of aging, was  
 405 measured in the three samples:

- 406 • 11.5 cm over a total of 20 cm (57%) in the SAT60% that underwent a maximal  
 407 temperature ( $T_{\max}$ ) of 70 °C (35 cycles);
- 408 • 9 cm over a total of 20 cm (45%) in the SAT60 % that underwent a  $T_{\max}$  of 80 °C  
 409 (83 cycles);
- 410 • 11 cm over a total of 20 cm (55%) for the SAT58% after 41 cycles until 70 °C and  
 411 10 cycles until 80 °C (52 cycles).

412 A reduction of the anhydrous sodium acetate volume and an increase of its porosity with a  
 413 higher temperature can first be qualitatively observed from Figure 16 (b). Indeed, the solubility of  
 414 sodium acetate increases with temperature, from 149 g/100 g of water at 72 °C to 154.3 g/100 g of  
 415 water at 83 °C [23]. After heating above 80 °C, the SAT60% (Figure 16 (b)) seems to contain a lower  
 416 quantity of segregated anhydrous salt (about 9 cm) than the SAT58% (11 cm, Figure 16 (c)). In  
 417 addition, the SAT60% appears more porous that may accentuate the difference between the heights  
 418 of segregated salts in both samples. Measuring the height of the segregated sample may help to  
 419 quantify aging. However, it should be used with caution, as a part of sodium acetate trihydrate may  
 420 be mixed with the porous anhydrous sodium acetate.

## 421 6. Conclusion and Outlook

422 This study was dedicated to the analysis of the aging of sodium acetate trihydrate. It was found  
 423 that the reference sample (SAT60%) had lost 10% of its latent heat quantity, from 235 to 215 J.g<sup>-1</sup> after  
 424 about 35 cycles. After such cycles, the evolution seemed asymptotic, reaching a constant value that  
 425 was supposed to be close to the final latent heat after aging. Besides, some crystallization occurred at  
 426 a lower temperature and were considered as singular behaviors. The supercooling degree of these  
 427 solidifications increased throughout cycles that may be considered as a factor of aging, unwanted for  
 428 applications. Indeed, a reduction of the SAT quantity at stoichiometric concentration would result in  
 429 a degradation of the properties. This would limit the use of this material as a storage medium.

430 Therefore, the addition of water as a solution to aging was investigated. In contrary to our  
 431 expectations, the sample containing water in excess (SAT58%) was less stable after 35 cycles. Indeed,  
 432 the latent heat had lost 25% of its initial value moving from about 225 to 170 J.g<sup>-1</sup>. In addition, the  
 433 achievement of the stability is slower, as the exponential fit gives a final value of 96 J.g<sup>-1</sup> (*vs* 213 J.g<sup>-1</sup>  
 434 for SAT60%).

435 Moreover, preliminary experiments have also shown that the agitation of the sample could  
 436 “reset” the value of latent heat. This agitation could be induced by any mechanical movements in the  
 437 liquid, such as shaking, bubbling, or ultrasound that may also present interest as nucleation

438 triggering techniques. Indeed, the limitation of the supercooling degree is generally targeted in phase  
439 change materials to improve their heat release capability.

440 Finally, for an application, the use of a high and narrow container could induce a more rapid  
441 aging behavior. Indeed, after the separation of the two species (sodium acetate and water) during  
442 heating, it may be more difficult to put them in contact during cooling. It would then be  
443 recommended to use a container of low height ( $h < 5$  cm) to limit the separation of species due to  
444 gravity in order to facilitate the rehydration of the SAT.

445 **Author Contributions:** Conceptualization, N.B., U.S., L.Z.; Methodology, N.B., U.S., L.Z.; Investigation, N.B.,  
446 L.Z.; Writing – Original Draft Preparation, N.B.; Writing – Review & Editing, N.B., U.S., L.Z.;

447 **Conflicts of Interest:** The authors declare no conflict of interest.

## 448 References

- 449 1. Systems & Components Available online: [http://comtes-](http://comtes-storage.eu/publications/presentations/development-line-c/systems-components/)  
450 [storage.eu/publications/presentations/development-line-c/systems-components/](http://comtes-storage.eu/publications/presentations/development-line-c/systems-components/) (accessed on 3  
451 September 2018).
- 452 2. Cabeza, L.F.; Castell, A.; Barreneche, C.; de Gracia, A.; Fernández, A.I. Materials Used as PCM in  
453 Thermal Energy Storage in Buildings: A Review. *Renew. Sustain. Energy Rev.* **2011**, *15*, 1675–1695,  
454 doi:10.1016/j.rser.2010.11.018.
- 455 3. Beaupere, N.; Soupremanien, U.; Zalewski, L. Nucleation Triggering Methods in Supercooled Phase  
456 Change Materials (PCM), a Review. *Thermochim. Acta* **2018**, *670*, 184–201,  
457 doi:10.1016/j.tca.2018.10.009.
- 458 4. Wada, T.; Kimura, F.; Matsuo, Y. Studies on Salt Hydrates for Latent Heat Storage. IV. Crystallization in  
459 the Binary System  $\text{CH}_3\text{CO}_2\text{Na}-\text{H}_2\text{O}$ . *Bull. Chem. Soc. Jpn.* **1983**, *56*, 3827–3829,  
460 doi:10.1246/bcsj.56.3827.
- 461 5. Beaupere, N.; Soupremanien, U.; Zalewski, L. Experimental Measurements of the Residual Solidification  
462 Duration of a Supercooled Sodium Acetate Trihydrate. *Int. J. Therm. Sci.* **2020**, *158*, 106544,  
463 doi:10.1016/j.ijthermalsci.2020.106544.
- 464 6. Mazzeo, D.; Oliveti, G.; de Gracia, A.; Coma, J.; Solé, A.; Cabeza, L.F. Experimental Validation of the  
465 Exact Analytical Solution to the Steady Periodic Heat Transfer Problem in a PCM Layer. *Energy* **2017**,  
466 *140*, 1131–1147, doi:10.1016/j.energy.2017.08.045.
- 467 7. Mazzeo, D.; Oliveti, G. Thermal Field and Heat Storage in a Cyclic Phase Change Process Caused by  
468 Several Moving Melting and Solidification Interfaces in the Layer. *Int. J. Therm. Sci.* **2018**, *129*, 462–488,  
469 doi:10.1016/j.ijthermalsci.2017.12.026.
- 470 8. Wada, T.; Yamamoto, R.; Matsuo, Y. Heat Storage Capacity of Sodium Acetate Trihydrate during  
471 Thermal Cycling. *Sol. Energy* **1984**, *33*, 373–375, doi:10.1016/0038-092X(84)90169-5.
- 472 9. Kong, W.; Dannemand, M.; Brinkø Berg, J.; Fan, J.; Englmaier, G.; Dragsted, J.; Furbo, S. Experimental  
473 Investigations on Phase Separation for Different Heights of Sodium Acetate Water Mixtures under  
474 Different Conditions. *Appl. Therm. Eng.* **2019**, *148*, 796–805, doi:10.1016/j.applthermaleng.2018.10.017.
- 475 10. Pálffy, E.G.; Prépostffy, E.; Zöld, A.; Bajnóczy, G. Thermal Properties of a Heat Storage Device  
476 Containing Sodium Acetate Trihydrate. *Period. Polytech. Chem. Eng.* **1995**, *39*, 129–135, doi:N/A.
- 477 11. Kong, W.; Dannemand, M.; Johansen, J.B.; Fan, J.; Dragsted, J.; Englmaier, G.; Furbo, S. Experimental  
478 Investigations on Heat Content of Supercooled Sodium Acetate Trihydrate by a Simple Heat Loss  
479 Method. *Sol. Energy* **2016**, *139*, 249–257, doi:10.1016/j.solener.2016.09.045.

- 480 12. Kong, W.; Dannemand, M.; Johansen, J.B.; Fan, J.; Dragsted, J.; Furbo, S. Ageing Stability of Sodium  
481 Acetate Trihydrate with and Without Additives for Seasonal Heat Storage. In Proceedings of the  
482 Proceedings of the ISES Solar World Congress 2015; International Solar Energy Society: Daegu, Korea,  
483 November 2016; pp. 1–10.
- 484 13. Furbo, S. Heat Storage with an Incongruently Melting Salt Hydrate as Storage Medium Based on the  
485 Extra Water Principle. In *Thermal Storage of Solar Energy*; Springer, Dordrecht, 1981; pp. 135–145  
486 ISBN 978-94-009-8304-5.
- 487 14. Dannemand, M.; Dragsted, J.; Fan, J.; Johansen, J.B.; Kong, W.; Furbo, S. Experimental Investigations  
488 on Prototype Heat Storage Units Utilizing Stable Supercooling of Sodium Acetate Trihydrate Mixtures.  
489 *Appl. Energy* **2016**, *169*, 72–80, doi:10.1016/j.apenergy.2016.02.038.
- 490 15. Dannemand, M.; Kong, W.; Fan, J.; Johansen, J.B.; Furbo, S. Laboratory Test of a Prototype Heat  
491 Storage Module Based on Stable Supercooling of Sodium Acetate Trihydrate. *Energy Procedia* **2015**,  
492 *70*, 172–181, doi:10.1016/j.egypro.2015.02.113.
- 493 16. Dannemand, M.; Johansen, J.B.; Kong, W.; Furbo, S. Experimental Investigations on Cylindrical Latent  
494 Heat Storage Units with Sodium Acetate Trihydrate Composites Utilizing Supercooling. *Appl. Energy*  
495 **2016**, *177*, 591–601, doi:10.1016/j.apenergy.2016.05.144.
- 496 17. Zalewski, L.; Franquet, E.; Gibout, S.; Tittlein, P.; Defer, D. Efficient Characterization of Macroscopic  
497 Composite Cement Mortars with Various Contents of Phase Change Material. *Appl. Sci.* **2019**, *9*, 1104,  
498 doi:10.3390/app9061104.
- 499 18. Desgrosseilliers, L. Design and Evaluation of a Modular, Supercooling Phase Change Heat Storage  
500 Device for Indoor Heating. Ph.D. Thesis, Université Dalhousie, 2017.
- 501 19. Dannemand, M. Compact Seasonal PCM Heat Storage for Solar Heating Systems. Ph.D. Thesis,  
502 Technical University of Denmark, 2015.
- 503 20. Ferrer, G.; Solé, A.; Barreneche, C.; Martorell, I.; Cabeza, L.F. Review on the Methodology Used in  
504 Thermal Stability Characterization of Phase Change Materials. *Renew. Sustain. Energy Rev.* **2015**, *50*,  
505 665–685, doi:10.1016/j.rser.2015.04.187.
- 506 21. Yehya, A. Contribution to the Experimental and Numerical Characterization of Phase-Change Materials :  
507 Consideration of Convection, Supercooling, and Soluble Impurities. Ph.D. Thesis, Université d'Artois,  
508 2015.
- 509 22. Beaupère, N. Pilotage de La Libération de Chaleur et Étude Du Vieillissement de Matériaux à  
510 Changement de Phase. Ph.D. Thesis, Université d'Artois, 2019.
- 511 23. Green, W.F. The "Melting-Point" of Hydrated Sodium Acetate: Solubility Curves. *J. Phys. Chem.* **1907**,  
512 *12*, 655–660, doi:10.1021/j150099a002.
- 513 24. Johansen, J.B.; Dannemand, M.; Kong, W.; Fan, J.; Dragsted, J.; Furbo, S. Thermal Conductivity  
514 Enhancement of Sodium Acetate Trihydrate by Adding Graphite Powder and the Effect on Stability of  
515 Supercooling. *Energy Procedia* **2015**, *70*, 249–256, doi:10.1016/j.egypro.2015.02.121.
- 516 25. Araki, N.; Futamura, M.; Makino, A.; Shibata, H. Measurements of Thermophysical Properties of Sodium  
517 Acetate Hydrate. *Int. J. Thermophys.* **1995**, *16*, 1455–1466, doi:10.1007/BF02083553.
- 518 26. Cabeza, L.F.; Roca, J.; Nogués, M.; Mehling, H.; Hiebler, S. Immersion Corrosion Tests on Metal-Salt  
519 Hydrate Pairs Used for Latent Heat Storage in the 48 to 58°C Temperature Range. *Mater. Corros.* **2002**,  
520 *53*, 902–907, doi:10.1002/maco.200290004.
- 521 27. Efremov, V.A.; Endeladze, N.O.; Agre, V.M.; Trunov, V.K. Refinement of the Crystal Structure of Sodium  
522 Acetate Trihydrate. *J. Struct. Chem.* **1986**, *27*, 498–501, doi:10.1007/BF00751841.

- 523 28. Duquesne, M.; Palomo Del Barrio, E.; Godin, A. Nucleation Triggering of Highly Undercooled Xylitol  
524 Using an Air Lift Reactor for Seasonal Thermal Energy Storage. *Appl. Sci.* **2019**, *9*, 267,  
525 doi:10.3390/app9020267.
- 526 29. Munakata, T.; Nagata, S. Electrical Initiation of Solidification and Preservation of Supercooled State for  
527 Sodium Acetate Trihydrate. In Proceedings of the 14th International Heat Transfer Conference, Volume  
528 7; ASME: Washington, DC, USA, August 2010; pp. 383–388.
- 529 30. Dannemand, M.; Delgado, M.; Lazaro, A.; Penalosa, C.; Gundlach, C.; Trinderup, C.; Johansen, J.B.;  
530 Moser, C.; Schranzhofer, H.; Furbo, S. Porosity and Density Measurements of Sodium Acetate  
531 Trihydrate for Thermal Energy Storage. *Appl. Therm. Eng.* **2018**, *131*, 707–714,  
532 doi:10.1016/j.applthermaleng.2017.12.052.
- 533 31. Guion, J.; Teisseire, M. Nucleation of Sodium Acetate Trihydrate in Thermal Heat Storage Cycles. *Sol.*  
534 *Energy* **1991**, *46*, 97–100, doi:10.1016/0038-092X(91)90021-N.
- 535 32. Zalba, B.; Marín, J.M.; Cabeza, L.F.; Mehling, H. Review on Thermal Energy Storage with Phase  
536 Change: Materials, Heat Transfer Analysis and Applications. *Appl. Therm. Eng.* **2003**, *23*, 251–283,  
537 doi:10.1016/S1359-4311(02)00192-8.
- 538 33. Wada, T. Study of Sodium Acetate Trihydrate for Latent Heat Storage. Thèse de doctorat, Osaka  
539 University, 1985.
- 540

541 **Publisher’s Note:** MDPI stays neutral with regard to jurisdictional claims in published maps and institutional  
542 affiliations.



© 2020 by the authors. Submitted for possible open access publication under the terms and conditions of the Creative Commons Attribution (CC BY) license (<http://creativecommons.org/licenses/by/4.0/>).

543